

PHYSICAL REVIEW B

CONDENSED MATTER

THIRD SERIES, VOLUME 53, NUMBER 10

1 MARCH 1996-II

RAPID COMMUNICATIONS

Rapid Communications are intended for the accelerated publication of important new results and are therefore given priority treatment both in the editorial office and in production. A Rapid Communication in Physical Review B may be no longer than four printed pages and must be accompanied by an abstract. Page proofs are sent to authors.

First-principles investigation of 180° domain walls in BaTiO_3

J. Padilla, W. Zhong, and David Vanderbilt

Department of Physics and Astronomy, Rutgers University, Piscataway, New Jersey 08855-0849

(Received 22 September 1995; revised manuscript received 21 December 1995)

We present a first-principles study of 180° ferroelectric domain walls in tetragonal barium titanate. The theory is based on an effective Hamiltonian that has previously been determined from first-principles ultrasoft-pseudopotential calculations. Statistical properties are investigated using Monte Carlo simulations. We compute the domain-wall energy, free energy, and thickness, analyze the behavior of the ferroelectric order parameter in the interior of the domain wall, and study its spatial fluctuations. An abrupt reversal of the polarization is found, unlike the gradual rotation typical of the ferromagnetic case.

The cubic perovskites are among the most important examples of ferroelectric materials.¹ Many undergo not just one, but a series, of structural phase transitions as the temperature is reduced. These transitions occur as a result of a delicate balance between long-range dipole-dipole interactions that favor the ferroelectric state, and short-range forces that favor the high-symmetry cubic perovskite phase. Because of the anomalously large Born effective charge of the atoms, the ferroelectric transitions in the perovskites are very sensitive to electrostatic boundary conditions.^{2,3} As a consequence, domain structure plays an important role in the ferroelectric transitions, and a theoretical understanding of the domain walls is of great interest.

Theoretical investigation of ferroelectric domain walls has been much less extensive than for their ferromagnetic counterparts. The strong coupling of ferroelectricity to structural and elastic properties is problematic. Previous theoretical investigations have concentrated on a phenomenological level of description, using Landau theory to study domain-wall thickness and energy.^{4,5} Simple microscopic models such as local-field theory have also been used to identify the domain-wall structure and character.⁶ Due to the limited experimental data available, this empirical work has tended to be qualitative and oversimplified and has thus not been able to offer the accuracy needed for a deeper theoretical understanding.

In this paper, we undertake a first-principles study of ferroelectric domain walls in BaTiO_3 . While several *ab initio* studies of bulk BaTiO_3 and related materials have ap-

peared in the literature,⁷⁻⁹ to our knowledge the present work is the first such study of the domain walls. Using an *ab initio* effective Hamiltonian developed previously to study the phase transitions of BaTiO_3 ,⁷ we set up Monte Carlo (MC) simulations to investigate the structure and energetics of 180° domain walls of (100) orientation. In particular, the energy, free energy, and thickness of the wall are calculated. We also analyze the behavior of the ferroelectric order parameter in the interior of the domain wall and study the fluctuations in the domain-wall shape. Where we can compare with previous work, we find our results in general agreement with experimental¹⁰⁻¹² and theoretical reports.

Because only low-energy distortions are important to the structural properties, we work with an effective Hamiltonian written in terms of a reduced number of degrees of freedom.⁷ The most important degrees of freedom included are the $3N$ "local-mode amplitudes" $u_{i\alpha}$ for site i and Cartesian direction α . A "site" is a primitive unit cell centered on a Ti atom, and the "local mode" on this site consists of displacements of the given Ti atom, its six nearest oxygen neighbors, and its eight nearest Ba neighbors, in such a way that a superposition of a uniform set of local-mode vectors $\mathbf{u}_i = \mathbf{e}$ (independent of i) generates the soft zone-center ferroelectric mode polarized along \hat{e} . We also include six degrees of freedom to represent homogeneous strain of the entire system and $3N$ displacement local-mode amplitudes $v_{i\alpha}$ that serve to introduce inhomogeneous strains. We thus reduce

the number of degrees of freedom per unit cell from 15 to 6, simplifying the expansion considerably.

Since the ferroelectric transition involves only small structural distortions, we represent the energy surface by a Taylor expansion around the high-symmetry cubic perovskite structure, including up to fourth-order anharmonic terms where appropriate. The energy consists of five parts: an on-site local-mode self-energy, a dipole-dipole interaction, a short-range interaction between local modes, an elastic energy, and a coupling between the elastic deformations and the local modes. The Hamiltonian is then specified by a set of expansion parameters, which are determined using highly accurate local-density approximation (LDA) calculations with Vanderbilt ultrasoft pseudopotentials.¹³ The details of the Hamiltonian, the first-principles calculations, and the values of the expansion parameters have been reported elsewhere.⁷ This scheme has been successfully applied to single-domain BaTiO₃ to predict the phase-transition sequence, transition temperatures, and other thermodynamic properties with good accuracy.

The phase-transition sequence for BaTiO₃ is cubic to tetragonal to orthorhombic to rhombohedral as temperature is reduced. We focus on the tetragonal phase, since it is the room-temperature phase, and the best studied experimentally. We adopt the convention that the polarization, and thus the tetragonal c axis, are along \hat{z} . In this phase, two kinds of domain walls, 90° and 180°, are possible.¹⁴ The notation refers to the angle between polarization vectors in adjacent domains. We choose the 180° domain wall for this study because of preliminary indications of a simple structure and narrow width.⁴ Because it is energetically unfavorable to form domain walls carrying net bound charge, 180° domain walls are restricted to lie parallel to the polarization. Earlier work has indicated that the 180° domain wall of (100) orientation has much lower energy than for other, e.g., (110), orientations.⁶ Thus, we focus on the (100) domain wall, which we take to lie in the y - z plane.

Ideally, we would like to study a single 180° domain wall in isolation. In order to make the simulation tractable, we apply artificial periodic boundary conditions. (While a study of a finite sample would also be interesting, the presence of surfaces would greatly complicate the analysis.) We use a $4L \times L \times L$ supercell (typically $L=10$) containing up and down domains alternating in the x direction. Thus, there are two 180° domain walls per supercell, with a spacing between walls of about 20 lattice constants. We find that this separation is more than enough to give converged results, based on tests of convergence with respect to L . In fact, previous work has indicated that the width of the 180° domain wall is very narrow, of the same order of magnitude as the lattice constant.^{4,6,10} Thus, in retrospect this should not be surprising.

For a very narrow domain wall, our choice of local mode (Ti centered as opposed to Ba centered) may introduce some bias. The point is that the sharpest domain wall that can be constructed is one for which the local-mode vectors \mathbf{u}_i are constant except for a sudden sign reversal from one plane of sites to the next. For the Ti centered choice of local modes, this represents a Ba-centered domain wall, for which the atomic displacements have odd symmetry across (and vanish on) the central Ba plane. Conversely, for a Ba-centered

choice of local mode, the sharpest domain wall is Ti centered, vanishing on a central plane of Ti atoms. In order to determine which of these scenarios is the more realistic, we constructed $4 \times 1 \times 1$ supercells (containing 20 atoms and 2 domain walls) corresponding to each of the above scenarios, using a mode amplitude taken from the average equilibrium structure of the MC simulations (very close to the experimental structure). We then performed LDA calculations to compare the energies of the two structures. We find the Ba-centered and Ti-centered walls constructed in this way have energies of 6.2 and 62.0 erg/cm², respectively. Thus, a sharp Ti-centered domain wall appears very unfavorable and it is clearly best to use a Ti-centered local mode as we have done. We note that the effective Hamiltonian reproduces the energy of this sharpest Ti-centered wall to within 1% of the LDA result (not surprisingly, since configurations of a similar kind were included in the fitting⁷).

We study the structure and energetics of the domain walls using Metropolis MC simulations.¹⁵ The degrees of freedom are the vectors \mathbf{u}_i and \mathbf{v}_i for each site i of the $4L \times L \times L$ supercell, and the six homogeneous strain components. As mentioned above, the supercell is arranged to contain two domains, each roughly of size $2L \times L \times L$, with domain walls normal to \hat{x} and with periodic boundary conditions. Since all energy contributions (except for the dipole-dipole coupling) are local, we choose the single-flip MC algorithm. We make a trial move of variables at one site, check acceptance, make the change if accepted, and go on to the next site. One Monte Carlo sweep (MCS) constitutes one entire pass through the system in this manner.

To generate a reasonable starting configuration for the $4L \times L \times L$ supercell, we equilibrate an $L \times L \times L$ supercell at a high temperature ($T > 400$ K) in the cubic phase and then cool it down slowly, allowing it to relax for 20 000 MCS's at each temperature step. We stop the cooling when the tetragonal phase is reached, in which the polarization vector averaged over the simulation cell points along one Cartesian axis. (As reported in Ref. 7, this phase corresponds to the temperature range from 230–290 K in our calculation, while the actual experimental range is 278–403 K.¹⁶) If the polarization is not along $+\hat{z}$, we rotate the structure to make it so. We then copy the structure four times along the x axis, with the polarization reversed to $-\hat{z}$ for two of them. The starting configuration thus contains two periodic 180° domain walls perpendicular to the (100) direction.

This structure is initially equilibrated for 2000 MCS's, in order to reach a good approximation to the “local equilibrium” associated with the presence of alternating domains. Thermodynamic averages are then constructed from runs of 40 000 MCS's. Of course the global equilibrium for our supercell would consist of a single-domain (bulk) structure; indeed, we find that fluctuations in the positions of the domain walls can occasionally cause two neighboring walls to touch, which leads rapidly to the mutual annihilation of the pair of walls. While this occurrence is fairly rare, we nevertheless decided to prevent it by fixing the z components of the \mathbf{u} vectors in the central two layers in each domain during the simulations, thus providing “barriers” to the motion of the domain walls. Since the domain walls are typically far from these barriers and the constrained structure is very close to the bulk equilibrium, we think the effect on our results is

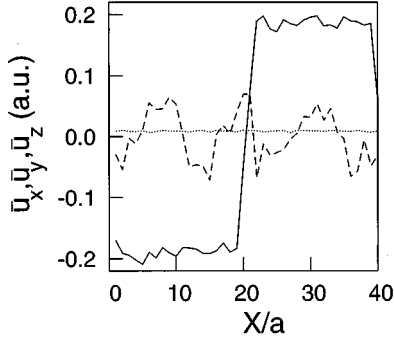


FIG. 1. Snapshot of the y - z layer-averaged polarization-vector components \bar{u}_x (dotted line), \bar{u}_y (dashed line), and \bar{u}_z (solid line), as a function of x/a (a is the lattice constant), for the $40 \times 10 \times 10$ lattice at 260 K.

negligible. Indeed, results taken from entirely unconstrained runs in which no annihilation event occurs appear very similar to those given below.

Figure 1 shows a snapshot of the polarization vector components averaged over y - z layers, \bar{u}_x , \bar{u}_y , and \bar{u}_z , as a function of x , for $L=10$. Several qualitative features are immediately apparent. First, the sharp reversal of u_z indicates that the domain boundary is indeed very sharp, its width being on the order of a lattice constant. Second, the other components u_x and u_y remain small throughout the whole supercell and their random fluctuations do not appear to be correlated with the domain-wall position. (The qualitative difference between the fluctuations of \bar{u}_x and \bar{u}_y with x is an artifact of the averaging and of the presence of strong longitudinal correlations.¹⁷) Thus, we find that the domain boundary entails a simple *reversal*, rather than a *rotation*, of the ferroelectric order parameter.

These behaviors are to be contrasted with the case of ferromagnetic domain walls, where the magnetization vector typically rotates gradually (on the atomic scale), keeping a roughly constant magnitude. This difference in behavior can probably be attributed largely to the much stronger strain coupling in the ferroelectric case. For our BaTiO_3 geometry, for example, the entire sample, including the interface, develops a tetragonal strain along \hat{z} , imposed by the presence of domains polarized along $\pm\hat{z}$. This gives rise to a strong anisotropy which will tend to keep the ferroelectric order parameter from developing components along x or y in the interface region. Thus, instead of rotating, the polarization simply decreases in magnitude and reverses as we pass through the domain wall. This absence of rotation of the polarization has been experimentally verified for the case of the 90° domain wall in BaTiO_3 .¹⁸

We now turn to a quantitative analysis of our simulation results, focusing on the domain-wall width, smoothness, and energy. We first estimate the domain-wall thickness t as follows. For a string of sites along x at a given value of (y,z) and on a given MCS, we identify the pair of sites between which u_z changes sign. We then define t via the linear extrapolation $t/a = 2u^{\text{spont}}/\Delta u_z$, where a is the lattice constant, u^{spont} is the spontaneous polarization deep in a domain, and Δu_z is the change of u_z between the two interface sites. Finally, we average over (y,z) points and over MCS's to get

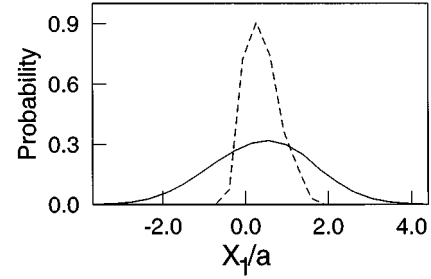


FIG. 2. Histograms of domain-wall positions for the $40 \times 10 \times 10$ lattice at 260 K. Solid line, histogram of $X_1(y,z,\tau)/a$ values (a is the lattice constant, τ labels a MCS); dashed line, histogram of y - z planar-average values $\bar{X}_1(\tau)/a$.

an average value of t . The value of t estimated in this way is 1.4 unit cells, or 5.6 Å. This is in reasonable agreement with empirical theoretical estimates of 6.7 Å (Ref. 5) and experiments which place an estimated upper bound of 50 Å.¹⁰

To analyze the smoothness of the domain wall, we Fourier transform the polarization u_z as a function of the x coordinate for each (y,z) point and retain only the first three terms in the expansion. This is an effective way to smooth the data while keeping the most useful information. The positions of the two domain walls in the supercell, denoted by X_1 and X_2 , are identified with the values of x at which the Fourier-smoothed u_z changes sign. In this way we obtain $X_1(y,z,\tau)$ and $X_2(y,z,\tau)$, where τ labels the MCS.

In Fig. 2, we show the probability distribution of X_1 for $L=10$ and for a run of 40 000 MCS's at 260 K. The solid line is a histogram of the values of $X_1(y,z,\tau)$, while the dashed line is a histogram of y - z planar averages $\bar{X}_1(\tau)$. A comparison of the two curves shows that the spatial fluctuations of the domain-wall position are much smaller than its ensemble fluctuations. From the solid line, we see that the X_1 values have a typical standard deviation of between one and two lattice constants. Other runs indicate that this result is not very sensitive to system size. So, we can conclude that the domain walls are relatively smooth. We can further separate the contributions to these fluctuations coming from the y and z directions. It is found that the fluctuations along the z direction (i.e., along the polar direction) are about 40% smaller than along the y direction. The sign of this result was to be expected, since the shape of the domain wall should be such as to minimize the surface charge $\Delta\mathbf{P}\cdot\mathbf{n}$ that develops on it. Here, $\Delta\mathbf{P}$ is the change of the polarization vector across the domain wall and \mathbf{n} is the unit vector normal to the wall.

Finally, we turn to an estimate of the domain-wall formation energy. Because of the periodic boundary conditions imposed on our system, there are no surfaces to give rise to a depolarization energy. Thus, the domain-wall energy E_w can be calculated from the difference between the energy of the $4L \times L \times L$ supercell with and without domain walls. This difference is small, but because the correlation time of the system (far from the transition) is quite short (20 MCS's), a sufficiently long simulation is capable of reducing the statistical errors in E_w to an acceptable level. The calculated domain-wall energies are shown in Table I. The reported values have a statistical uncertainty of about 4%. Simulations

TABLE I. Calculated domain-wall energies E_w and free energies F_w as a function of simulation cell size L and temperature T . Statistical uncertainties are about 4% for E_w and 10% for F_w .

T (K)	L	E_w (erg/cm ²)	F_w (erg/cm ²)
250	8	15.8	4.6
260	8	17.1	4.0
250	10	15.6	5.0
260	10	17.0	4.4

for two lattice sizes and temperatures are reported. We can see that our results are well converged with respect to system size. Because of the large increase of the correlation time near the transitions, it has proven difficult to give accurate values for E_w at other temperatures.

Our calculated value of $E_w=16$ erg/cm² for the domain-wall energy is, however, probably not the proper quantity to compare with experimentally derived values. Instead, we should compute a *free energy*, F_w , which includes entropic contributions from fluctuations of the ferroelectric order parameter in the vicinity of the domain wall. A glance at Fig. 1, which shows considerable fluctuations, suggests that such contributions are likely to be important.

We have estimated the domain-wall free energies F_w using an adiabatic switching technique, as follows. First, we start with an equilibrated $4L \times L \times L$ supercell containing two domain walls, and for which the z components of the \mathbf{u} vectors in the central two layers in each domain are constrained to preset values, as before. We slowly reverse the values of the constraint variables in the center of one of the domains over the course of a 20 000-MCS simulation, making a small change in the constraint variables every 10 MCS's, and compute the total work done on the constraint variables. If the simulation succeeds in removing the two domain walls adiabatically, we can equate the work done to twice the domain-wall free energy F_w . By comparing runs of from 20 000 to 30 000 MCS's, we find differences in computed F_w values of only about 10%, which suggests that the switching is indeed adiabatic. The resulting computed values of F_w are about 4–5 erg/cm², or about 3–4 times smaller than the E_w values (and slightly smaller than the 6.2 erg/cm² reported above for the energy of the ideal Ba-centered wall).

Our result is consistent with previously published estimates of the “energy” of the (100) 180° domain wall, although such previous values are rather scattered and inconclusive. Previous experimental results of 10 and 3 erg/cm² (close to the phase transition) were given by Merz¹¹ and Fousek and Safrankova,¹² respectively. On the theoretical side, Bulaevskii⁵ reported a value of 10.5 erg/cm² using a continuum Landau p^6 model, while Lawless⁶ calculated an energy of 1.52 erg/cm² based on a microscopic phenomenological model. (Since the above estimates involve use of empirical models fit to finite-temperature data, the “energy” values are probably best interpreted as free energies.)

This investigation has opened several avenues for further study. One important goal is to apply the model to more realistic geometries that include surfaces; after all, in real samples the domain structure generally arises because of the depolarization energy associated with surfaces. A natural first step would be to consider a slab geometry, to make contact with experimental thin-film studies. This would require first-principles calculations of very thin slabs (~ 3 – 5 unit cells thick) to determine the necessary modifications to the effective Hamiltonian at the surface, followed by Monte Carlo simulations on thicker slabs containing ferroelectric domains. We are now beginning to undertake first-principles calculations of the type needed. Other interesting avenues would be to study other types of domain walls [e.g., (110) 180° or 90° domain walls] in tetragonal BaTiO₃ and to consider other phases of BaTiO₃ or other perovskite materials.

In summary, we have studied the properties of 180° domain walls in BaTiO₃ using a first-principles based approach, by applying Monte Carlo simulations to a microscopic effective Hamiltonian that was fitted to *ab initio* total-energy calculations. The simulations were carried out in the middle of the temperature region of the tetragonal phase, relatively far from the C - T and T - O transitions. We confirm that the domain walls are atomically thin and that the order parameter does not rotate within the wall. We quantify the width, smoothness, and energetics of these domain walls. Our theoretical values of the wall width and free energy are in reasonable agreement with previously reported values, where available.

This work was supported by the Office of Naval Research under contract number N00014-91-J-1184.

¹M. E. Lines and A. M. Glass, *Principles and Applications of Ferroelectrics and Related Materials* (Clarendon, Oxford, 1977).

²R. Resta, M. Posternak, and A. Baldereschi, *Phys. Rev. Lett.* **70**, 1010 (1993).

³W. Zhong, R. D. King-Smith, and D. Vanderbilt, *Phys. Rev. Lett.* **72**, 3618 (1994).

⁴V. A. Zhirnov, *Sov. Phys. JETP* **35**, 822 (1959).

⁵L. N. Bulaevskii, *Sov. Phys. Solid State* **5**, 2329 (1964).

⁶W. N. Lawless, *Phys. Rev.* **175**, 619 (1968).

⁷W. Zhong, D. Vanderbilt, and K. M. Rabe, *Phys. Rev. Lett.* **73**, 1861 (1994); *Phys. Rev. B* **52**, 6301 (1995).

⁸R. E. Cohen and H. Krakauer, *Phys. Rev. B* **42**, 6416 (1990); *Ferroelectrics* **136**, 65 (1992); R. E. Cohen, *Nature* **358**, 136 (1992).

⁹D. J. Singh, *Ferroelectrics* **164**, 143 (1995).

¹⁰M. Tanaka and G. Honjo, *J. Phys. Soc. Jpn.* **19**, 954 (1964).

¹¹W. J. Merz, *Phys. Rev.* **95**, 690 (1954).

¹²J. Fousek and M. Safrankova, *Jpn. J. Appl. Phys.* **4**, 403 (1965).

¹³D. Vanderbilt, *Phys. Rev. B* **41**, 7892 (1990).

¹⁴J. Fousek and V. Janovec, *J. Appl. Phys.* **40**, 135 (1969).

¹⁵*The Monte Carlo Method in Condensed Matter Physics*, edited by K. Binder (Springer-Verlag, Berlin, 1992).

¹⁶T. Mitsui *et al.*, in *Ferroelectrics and Related Substances. Oxides*, edited by O. Madelung, Landolt-Börnstein, New Series, Group 3, Vol. 16, Pt. a (Springer-Verlag, Berlin, 1981).

¹⁷The strong dipolar interactions give rise to a strong longitudinal correlation of the \mathbf{u}_i . That is, u_x is strongly correlated along

x , while u_y is strongly correlated along y . The averaging over y - z planes involved in the definition of \bar{u} thus amplifies the fluctuations of \bar{u}_y , while suppressing those of \bar{u}_x .

¹⁸S. I. Yakunin, V. V. Shakmanov, G. V. Spivak, and N. V. Vasileva, *Sov. Phys. Solid State* **14**, 310 (1972).